

# Collapse of a molecular cloud core to stellar densities: the radiative impact of stellar core formation on the circumstellar disc

Matthew R. Bate<sup>\*</sup>

*School of Physics, University of Exeter, Stocker Road, Exeter EX4 4QL*

22 October 2021

## ABSTRACT

We present results from the first three-dimensional radiation hydrodynamical calculations to follow the collapse of a molecular cloud core beyond the formation of the stellar core. We find the energy released by the formation of the stellar core, within the optically-thick first hydrostatic core, is comparable to the binding energy of the disc-like first core. This heats the inner regions of the disc, drives a shock wave through the disc, dramatically decreases the accretion rate on to the stellar core, and launches a temporary bipolar outflow perpendicular to the rotation axis that travels in excess of 50 AU into the infalling envelope.

This outburst may assist the young protostar in launching a conventional magnetic jet. Furthermore, if these events are cyclic, they may provide a mechanism for intense bursts of accretion separated by long periods of relatively quiescent accretion which can potentially solve both the protostellar luminosity problem and the apparent age spread of stars in young clusters. Such outbursts may also provide a formation mechanism for the chondrules found in meteorites, with the outflow transporting them to large distances in the circumstellar disc.

**Key words:** accretion, accretion discs – hydrodynamics – radiative transfer – stars: formation – stars: low-mass, brown dwarfs – stars: winds, outflows.

## 1 INTRODUCTION

More than four decades ago, Larson (1969) performed the first numerical calculations of the collapse of a molecular cloud core to stellar core formation and beyond. These one-dimensional radiation hydrodynamical calculations revealed the main stages of protostar formation: an almost isothermal collapse until the inner regions become optically thick, the almost adiabatic formation of the first hydrostatic core (typical radius  $\approx 5$  AU and initial mass  $\approx 5 M_J$ ), the growth of this core as it accreted from the infalling envelope, the second collapse within this core triggered by the dissociation of molecular hydrogen, the formation of the stellar core (initial radius  $\approx 2 R_\odot$  and mass  $\approx 1.5 M_J$ ), and, lastly, the long accretion phase of the stellar core to its final mass. Subsequent one-dimensional (e.g. Masunaga & Inutsuka 2000) and two-dimensional (Tscharnutter 1987; Tscharnutter et al. 2009) calculations have not changed this qualitative picture substantially, although the latter have allowed the disc-like structure of rotating first cores to be studied.

The first three-dimensional hydrodynamical calculations to follow the collapse to stellar core formation were performed more than a decade ago by Bate (1998). These calculations of rotating molecular cloud cores examined the non-axisymmetric evolution of the first core and the second collapse phase. If the first core was rotating rapidly enough it was found to be dynamically unstable to a bar-mode leading to the formation of trailing spiral arms.

Gravitational torques removed angular momentum and rotational support from the inner regions of the first core, quickening the onset of the second collapse and preventing fragmentation during the second collapse phase to form close binaries. Several subsequent studies have investigated this phenomenon in more detail (Saigo & Tomisaka 2006; Saigo, Tomisaka & Matsumoto 2008; Machida, Inutsuka & Matsumoto 2010), some also including magnetic fields and finding outflows (Machida et al. 2005, 2006). However, all these calculations used barotropic equations of state rather than solve the radiation hydrodynamical problem.

The first three-dimensional calculations including radiative transfer that followed collapse to the point of stellar core formation (but not beyond) were Whitehouse & Bate (2006), using the flux-limited diffusion approximation, and Stamatellos et al. (2007), using a radiative cooling approximation. Most recently, radiation magnetohydrodynamical calculations of cloud collapse have been performed (Tomida et al. 2010), but were stopped before the onset of the second collapse.

In this paper, we report results from the first three-dimensional radiation hydrodynamical calculations to follow the collapse of rotating molecular cloud cores *beyond* the formation of the stellar core. We find that the use of radiation hydrodynamics rather than a barotropic equation of state has little effect up until the formation of the stellar core. However, with radiative transfer, the energy released by the formation of the stellar core has a dramatic effect on the surrounding disc and envelope and launches a temporary outflow *even in the absence of a magnetic field*.

<sup>\*</sup> E-mail: mbate@astro.ex.ac.uk

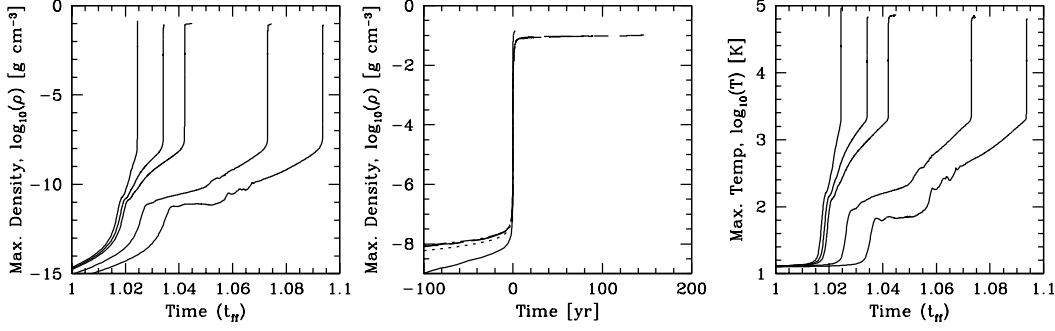


**Figure 1.** The time evolution of the maximum (central) density (left two panels) and temperature (right panel). For the left and right panels, the lines are for cloud cores with  $\beta = 0, 5 \times 10^{-4}, 0.001, 0.005, 0.01$  from left to right. For the central panel, for each calculation the time in years has been zeroed when the density first exceeded  $10^{-3} \text{ g cm}^{-3}$  and the  $\beta = 0$  calculation is plotted with a solid line,  $\beta = 5 \times 10^{-4}$  with a dotted line, and the other calculations are indistinguishable. The free-fall time of the initial cloud core,  $t_{\text{ff}} = 1.8 \times 10^{12} \text{ s}$  (56,500 yrs). Each calculation was performed with  $10^6$  SPH particles.

## 2 COMPUTATIONAL METHOD

The calculations presented here were performed using a three-dimensional smoothed particle hydrodynamics (SPH) code based on the original version of Benz (1990; Benz et al. 1990), but substantially modified as described in Bate et al. (1995), Whitehouse, Bate & Monaghan (2005), Whitehouse & Bate (2006), Price & Bate (2007), and parallelised using both OpenMP and MPI.

Gravitational forces between particles and a particle's nearest neighbours are calculated using a binary tree. The smoothing lengths of particles are variable in time and space, set iteratively such that the smoothing length of each particle  $h = 1.2(m/\rho)^{1/3}$  where  $m$  and  $\rho$  are the SPH particle's mass and density, respectively (see Price & Monaghan 2007, for further details). The SPH equations are integrated using a second-order Runge-Kutta-Fehlberg integrator with individual time steps for each particle (Bate et al. 1995). To reduce numerical shear viscosity, we use the Morris & Monaghan (1997) artificial viscosity with  $\alpha_v$  varying between 0.1 and 1 while  $\beta_v = 2\alpha_v$  (see also Price & Monaghan 2005).

### 2.1 Equation of state and radiative transfer

We use an ideal gas equation of state  $p = \rho T \mathcal{R} / \mu$ , where  $T$  is the gas temperature,  $\mathcal{R}$  is the gas constant, and  $\mu$  is the mean molecular mass. The equation of state takes into account the translational, rotational, and vibrational degrees of freedom of molecular hydrogen (assuming a 3:1 mix of ortho- and para-hydrogen; see Boley et al. 2007). It also includes molecular hydrogen dissociation, and the ionisations of hydrogen and helium. The hydrogen and helium mass fractions are  $X = 0.70$  and  $Y = 0.28$ , respectively. The contribution of metals to the equation of state is neglected. Two temperature (gas and radiation) radiative transfer in the flux-limited diffusion approximation is implemented as described by Whitehouse et al. (2005) and Whitehouse & Bate (2006), except that the standard explicit SPH contributions to the gas energy equation due to the work and artificial viscosity are used when solving the (semi-)implicit energy equations to provide better energy conservation. We assume solar metallicity gas, using the interstellar grain opacity tables of Pollack et al. (1985) and the gas opacity tables of Alexander (1975) (the IVa King model) (see Whitehouse & Bate 2006).

### 2.2 Initial conditions

The initial conditions for the calculations are identical to those of Bate (1998). We follow the collapse of initially uniform-density,

uniform-rotating, molecular cloud cores of mass  $M = 1 M_{\odot}$  and radius  $R = 7 \times 10^{16} \text{ cm}$ . The ratios of the thermal and rotational energies to the magnitude of the gravitational potential energy are  $\alpha = 0.54$  and  $\beta$ , respectively. We have performed calculations with  $\beta = 0$  (not rotating), and  $\beta = 5 \times 10^{-4}, 0.001, 0.005$  and  $0.01$ .

To satisfy the resolution criterion of Bate & Burkert (1997) that the minimum Jeans mass during the calculation contains at least  $\approx 2N_{\text{neigh}} = 100$  particles, we require at least  $1 \times 10^5$  equal-mass particles. To test for convergence, we performed calculations using  $1 \times 10^5, 3 \times 10^5, 1 \times 10^6$ , and  $3 \times 10^6$  equal-mass SPH particles. The calculations were performed on the University of Exeter Supercomputer, an SGI Altix ICE 8200.

## 3 RESULTS

The collapse of the molecular cloud cores up until the formation of the stellar core proceeds in a manner very similar to that reported from previous three-dimensional calculations using barotropic equations of state (Bate 1998; Saigo & Tomisaka 2006; Saigo et al. 2008; Machida et al. 2010). Fig. 1, gives the evolution of the maximum density and temperature for the  $10^6$  particle calculations with different initial rotation rates. The initial collapse is almost isothermal until the maximum density exceeds  $\approx 10^{-13} \text{ g cm}^{-3}$ . As the central regions of the cloud become optically thick, the gas begins to trap the radiation and the collapse enters an almost adiabatic phase where the temperature rises as the gas is compressed. This leads to the formation of a pressure-supported ‘first core’ (Larson 1969), which can be seen in Fig. 1 when the initial collapse stalls with central (maximum) densities  $\sim 10^{-11} \text{ g cm}^{-3}$  and temperatures of  $\approx 70 - 120 \text{ K}$ , depending on the degree of rotational support (i.e. cores that rotate more quickly have lower central temperatures). Without rotation, the first core has an initial mass of  $\approx 5$  Jupiter masses ( $M_J$ ) and a radius of  $\approx 5 \text{ AU}$ . However, with higher initial rotation rates of the molecular cloud core, the first cores become progressively more oblate. For example, with  $\beta = 0.005$  before the onset of dynamical instability, the first core has a radius of  $\approx 20 \text{ AU}$  and a major to minor axis ratio of  $\approx 4:1$  (left panels, Fig. 2). Thus, for the higher rotation rates, the first core is actually a disc, but without a central object. As pointed out by Bate (1998) and Machida et al. (2010), in these cases the disc actually forms *before* the star.

The subsequent evolution of the first core depends on its rotation rate. Non-rotating and slowly rotating cores evolve as they accrete mass from the surrounding infalling envelope with their cen-

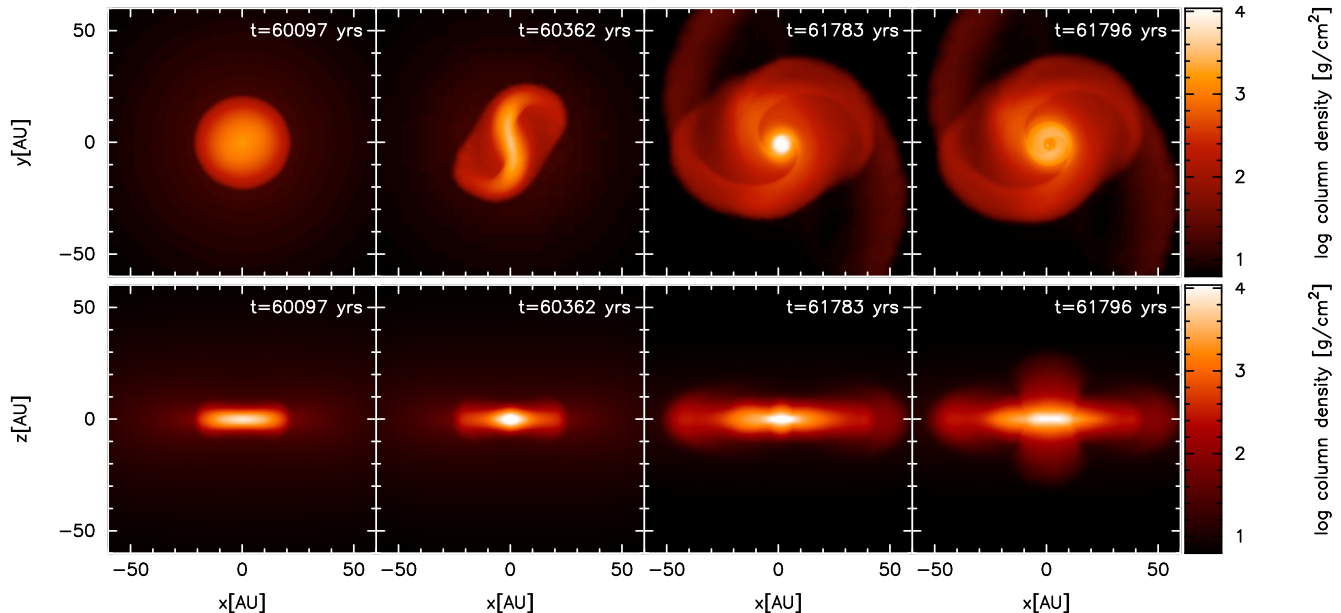


**Figure 2.** Column density images of the evolution of the first core, shock wave, and outflow for the  $\beta = 0.005$  case (using  $3 \times 10^6$  SPH particles). The rapidly rotating first core is highly oblate (left panels) and undergoes a dynamical bar-mode instability (centre-left panels) which transports angular momentum out of the centre, transforms the core into a disc, and triggers the formation of the stellar core. The energy released by stellar core formation heats the inner regions of the disc and drives a shock wave through the disc (upper right two panels) and a bipolar outflow perpendicular to the disc (lower right two panels). Animations can be found at <http://www.astro.ex.ac.uk/people/mbate/Animations/Stellar/>.

tral densities and temperatures increasing (Fig. 1, calculations with  $\beta \leq 0.001$ ). When the central temperatures of a first core exceeds  $\approx 2000$  K, molecular hydrogen begins to dissociate, absorbing energy and leading to a second hydrodynamic collapse deep within the first core. The collapse continues until the molecular hydrogen has been complete dissociated at the centre of the core where upon a second pressure-supported core begins to form, the ‘stellar’ core (Larson 1969). The formation of the stellar core occurs just a few years after the onset of the second collapse, during which the maximum density increases from  $\sim 10^{-8}$  to  $\approx 0.1 \text{ g cm}^{-3}$  and the maximum temperature increases from 2000 to  $> 60,000$  K. The stellar core is formed with a mass of  $M_{\text{sc}} \approx 1.5 \text{ M}_{\text{J}}$  and a radius of  $R_{\text{sc}} \approx 2 \text{ R}_{\odot}$ . Without rotation, the stellar core accretes the remnant of the first core in which it is embedded in  $\approx 10$  yr and then accretes the envelope (Larson 1969).

If the first core is rotating rapidly enough that its value of  $\beta > 0.274$ , the core is dynamically unstable to the growth of non-axisymmetric structure (Bate 1998). For the particular initial conditions used here, this occurs for the  $\beta = 0.005$  (see Fig. 2) and  $\beta = 0.01$  cases. The first core develops a bar-mode, and then spiral structure as the ends of the bar wind up (e.g. Durisen et al. 1986; Bate 1998). The spiral structure removes angular momentum from the inner parts of the first core, the effect of which can be seen in the evolution of density and temperature in Fig. 1. Specifically, for the  $\beta = 0.005$  case, the slow increase in central density and temperature accelerate with the onset of the spiral structure at  $t = 1.05 t_{\text{ff}}$ . This substantially accelerates the evolution of the first core towards the second collapse, which would have taken much longer to reach without the angular momentum redistribution. It also inhibits fragmentation during the second collapse phase because the gas undergoing the second collapse has less angular momentum than it would otherwise (Bate 1998). When the stellar core forms it is *already surrounded by a large disc* (radius  $\approx 50$  AU; Fig. 2) which

is the remnant of the gravitationally-unstable first core (Bate 1998; Machida et al. 2010).

For even higher rotation rates of the initial molecular cloud core ( $\beta \gtrsim 0.02$ ), the first core is actually a ring-like structure (e.g. Norman & Wilson 1978; Cha & Whitworth 2003) which is prone to dynamical fragmentation into two or more objects, each of which evolves in a similar manner to the more slowly rotating first cores.

As mentioned at the start of this section, all of this evolution with radiation hydrodynamics is almost identical to the evolution that is obtained when using a barotropic equation of state. The small differences that are found will be discussed in a separate paper. The main purpose of this letter is to discuss the evolution subsequent to the formation of the stellar core, which is *qualitatively different* to that obtained with a barotropic equation of state.

### 3.1 The effect of stellar core formation

When using a barotropic equation of state, the formation of the stellar core deep within the optically-thick disc has no effect on the temperature of the majority of the gas in the disc because the temperature is set purely according to the density of the gas. However, with radiation hydrodynamics, the situation is completely different.

When the second collapse occurs and produces the stellar core, the gravitational potential energy that is released is  $\sim GM_{\text{sc}}^2/R_{\text{sc}} = 4 \times 10^{42}$  erg. Since the stellar core is in virial equilibrium, approximately half of this energy is to be radiated away. Moreover, the stellar core rapidly begins to accrete from the first core, reaching a mass of  $\approx 6 \text{ M}_{\text{J}}$  in only a few years (i.e. more quickly than the dynamical timescale of the disc; see below). This increases the total energy released to  $\approx 3 \times 10^{43}$  erg. However, the binding energy of the disc in the  $\beta = 0.005$  calculation, for example, calculated just before the onset of the second collapse (i.e. the binding energy of the gas surrounding the stellar core that makes up the disc) is only  $4 \times 10^{43}$  erg (which can be estimated as

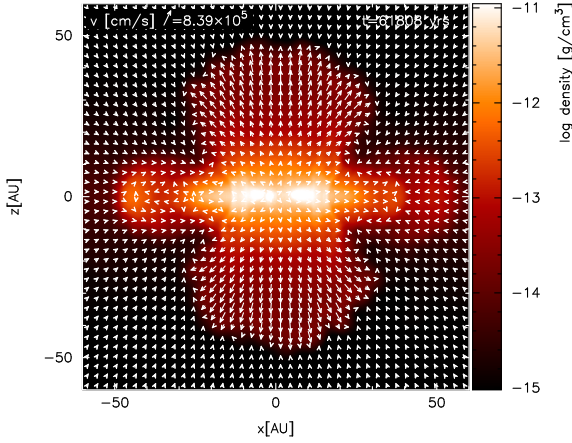


**Figure 3.** A cross section down the rotation axis ( $x - z$  plane) of the  $\beta = 0.005$  calculation with  $3 \times 10^6$  particles showing the density (colour scale) and velocities (vectors). The bipolar outflow is clearly visible and has travelled 50 AU into the surrounding infalling envelope only 35 yr after stellar core formation. The shock wave travelling along the midplane of the disc has propagated 17 AU out into the disc in the same period of time. Animations can be found at <http://www.astro.ex.ac.uk/people/mbate/Animations/Stellar/>.

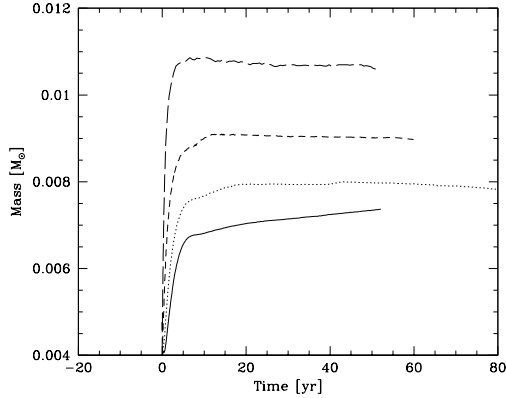


**Figure 4.** The mass of the stellar core (gas with density  $> 10^{-4} \text{ g cm}^{-3}$ ) measured from the time of its formation for the  $\beta = 0.005$  molecular cloud core performed using  $10^5$  (long-dashed line),  $3 \times 10^5$  (short-dashed line),  $10^6$  (dotted line), and  $3 \times 10^6$  (solid line) particles. With low resolution the radiative feedback stops accretion onto the stellar core, but for the highest resolution the accretion continues at a low level ( $10^{-5} \text{ M}_\odot \text{ yr}^{-1}$ ).

$\sim GM_d^2/R_d$  with  $M_d \approx 0.18 \text{ M}_\odot$  and taking a mean ‘spherical’ radius of  $R_d \approx 15 \text{ AU}$ ). Thus, the disc suddenly finds itself irradiated from the inside by an energy source emitting a substantial fraction of the binding energy of the disc itself. Because the disc is extremely optically thick, this energy is temporarily trapped in the centre of the disc and heats the gas dramatically, sending a weak shock wave (Mach number  $\approx 1$ ) out along the midplane of the disc (initial speed  $\approx 2 \text{ km s}^{-1}$ ). However, perpendicular to the disc, the effect is even more dramatic. Because there is less material along the rotation axis, the hot gas finds it easiest to break out in this direction and a bipolar outflow is launched. Whereas the wave within the disc decays as it travels leaving the bulk of the disc gravitationally bound, the gas forming the bipolar outflow has velocities in excess of  $8 \text{ km s}^{-1}$  and travels out into the infalling envelope to distances in excess of 50 AU in less than 50 years (Figs. 2 and 3).

The energy released by stellar core formation is somewhat dependent on the resolution of the calculations because the heating and outflow inhibit accretion onto the stellar core, which in turn results in less energy being released. Thus, the higher the resolution, the quicker the radiative feedback is able to inhibit the accretion and, therefore, the lower the initial mass of the stellar core. In Fig. 4, we plot the mass with density  $> 10^{-4} \text{ g cm}^{-3}$  versus time for the  $\beta = 0.005$  case with resolutions ranging from  $10^5$  to  $3 \times 10^6$  SPH particles. It can be seen that the mass of the stellar core at which the feedback dramatically curtails the accretion decreases from  $\approx 11$  to  $6 \text{ M}_J$  with increased resolution. For a few years, the stellar core grows at a rate of  $\sim 10^{-3} \text{ M}_\odot \text{ yr}^{-1}$  (even with the highest resolution). With low-resolution ( $\leq 1 \times 10^5$  SPH particles), the accretion onto the stellar core actually ceases entirely during the launching of the outflow. However, using  $3 \times 10^6$  SPH particles, we find that the stellar core does continue to grow during this time, but at a much reduced accretion rate of  $1 \times 10^{-5} \text{ M}_\odot \text{ yr}^{-1}$  (measured between 20 and 50 years after stellar core formation; Fig. 4). Although convergence with increasing resolution is relatively slow, a strong outflow is launched in all cases.

#### 4 DISCUSSION

These first calculations raise many questions to be followed up in the future. First, although the outflow seen in the calculations discussed here is transient and cannot be the origin of protostellar jets or outflows, such heating upon stellar core formation might aid in the launching of a magnetic jet by helping to clear material perpendicular to the disc and combining substantial thermal support with magnetic support. Therefore, using future radiation magnetohydrodynamical calculations it will be important to assess the relative roles of the radiative impact of stellar core formation and magnetic fields in the launching of the protostellar jet. Similarly, it would be desirable to resolve the accretion shock at the surface of the stellar core and to use a radiative transfer method that treats the optically-thin regime better than the flux-limited diffusion approximation.

Second, although the dramatic decrease in the stellar core accretion rate is also a transient, the question arises as to whether such a situation might be cyclic. One can imagine that after the disc settles down again, the accretion rate on to the stellar core may increase, leading to a repeat of the rapid accretion, the generation of a large accretion luminosity, the strengthening of an outflow and heating of the disc, and the consequential decrease in the stellar core’s accretion rate. The driving mechanism for the increased stellar accretion rate could be the redevelopment of spiral density waves in the disc as it recovers from the previous shock wave (Fig. 2). Such gravitational instabilities have been invoked to argue that accretion in the early Class 0 and I stages of star formation may be highly variable (Vorobyov & Basu 2005, 2006). The stellar accretion luminosity may then provide a way to temporarily switch the gravitational instability off. Another possible mechanism for variable accretion might be a mismatch between the accretion rates given by gravitational instability at large radii and the magnetorotational instability at small radii (Armitage et al. 2001; Zhu et al. 2009). If most of a star’s mass is accumulated in short bursts of intense accretion, this can potentially explain the observation that protostars are observed to be less luminous than expected for steady accretion (see Kenyon et al. 1990; Hartmann & Kenyon 1996), and also the apparent age spread of young stars in the Hertzsprung-Russell diagram (see Baraffe, Chabrier & Gallardo 2009).

Finally, there is the age old problem of how the chondrules

found in meteorites were formed (Grossman et al. 1988) as their production is thought to require high temperatures ( $> 1500$  K). Although many theories have been advanced in order to explain chondrule formation (see, for example, the review by Boss 1996), there is still no widely accepted mechanism. In this context, it is of interest to note that the temperatures within  $\approx 3$  AU of the stellar core at the launching of the outflows exceed 1500 K. While most of this material is no doubt be accreted by the star, a fraction produces the outflows which reach beyond 50 AU. If chondrules were formed in this outburst event, some might be entrained in the outflow and eventually fall back into the circumstellar disc at large distances from the star. Again, if such events were cyclic this would help because chondrule formation is thought to have occurred over several million years (Scott 2007).

## 5 CONCLUSIONS

We have presented results from the first three-dimensional radiation hydrodynamical calculations to follow the collapse of a molecular cloud core beyond the formation of the stellar core. We find the evolution before the formation of the stellar core is very similar to that found in the past using barotropic equations of state. In particular, the evolution of the first hydrostatic core which, depending on its rotation rate, may be dynamically unstable to the growth of non-axisymmetric perturbations and the generation of spiral structure, is very similar to that found in barotropic calculations. As found in earlier calculations, a rapidly rotating first core actually evolves into a disc so that the disc actually forms *before* the stellar core.

However, we find that the evolution following the formation of the stellar core is *qualitatively* different in radiation hydrodynamical calculations. In barotropic calculations, the formation of the stellar core deep inside the first core (or disc) has no effect on the surrounding disc because the temperature of the gas is simply set by the density of the gas. However, with radiation hydrodynamics, the energy released by the formation of the stellar core within the optically thick disc is similar to the binding energy of the disc. This heats the inner regions of the disc, drives a shock wave outwards through the disc, dramatically decreases the accretion rate on to the stellar core, and launches a bipolar outflow perpendicular to the rotation axis that can travel in excess of 50 AU out into the infalling envelope in less than 50 years.

We speculate that such outflows may assist the young protostar in launching a conventional magnetic jet by clearing a path perpendicular to the disc and adding substantial thermal pressure to the force provided by the magnetic field. It may also be that such events are cyclic, occurring every time the accretion rate onto the protostar exceeds a certain level rather than simply being a one-off event associated with the formation of the stellar core. If so, such events may provide the mechanism for intense bursts of accretion separated by long periods of relatively quiescent accretion which may be necessary to solve the protostellar luminosity problem and the apparent age spread of young stars. Finally, such outbursts may provide another mechanism for the formation of chondrules in meteorites and the associated outflows may be able to transport them to large distances in the circumstellar disc.

## ACKNOWLEDGMENTS

The computations were performed using the University of Exeter Supercomputer. Figs. 2 and 3 were produced using the publicly

available SPLASH visualisation software (Price 2007). This work, conducted as part of the award “The formation of stars and planets: Radiation hydrodynamical and magnetohydrodynamical simulations” made under the European Heads of Research Councils and European Science Foundation EURYI (European Young Investigator) Awards scheme, was supported by funds from the Participating Organisations of EURYI and the EC Sixth Framework Programme.

## REFERENCES

- Alexander D. R., 1975, *ApJS*, 29, 363
- Armitage P. J., Livio M., Pringle J. E., 2001, *MNRAS*, 324, 705
- Baraffe I., Chabrier G., Gallardo J., 2009, *ApJ*, 702, L27
- Bate M. R., 1998, *ApJ*, 508, L95
- Bate M. R., Bonnell I. A., Price N. M., 1995, *MNRAS*, 277, 362
- Bate M. R., Burkert A., 1997, *MNRAS*, 288, 1060
- Benz W., 1990, in Buchler J. R., ed., *Numerical Modelling of Nonlinear Stellar Pulsations Problems and Prospects*. Kluwer, Dordrecht, p. 269
- Benz W., Cameron A. G. W., Press W. H., Bowers R. L., 1990, *ApJ*, 348, 647
- Boley A. C., Hartquist T. W., Durisen R. H., Michael S., 2007, *ApJ*, 656, L89
- Boss A. P., 1996, in Hewins R. H., Jones R. H., Scott E. R. D., eds, *Chondrules and the Protoplanetary Disk*. Cambridge Univ. Press, Cambridge, p. 257
- Cha S., Whitworth A. P., 2003, *MNRAS*, 340, 91
- Durisen R. H., Gingold R. A., Tohline J. E., Boss A. P., 1986, *ApJ*, 305, 281
- Grossman J. N., Rubin A. E., Nagahara H., King E. A., 1988, in Kerridge J. F., Matthews M. S., eds, *Meteorites and the Early Solar System*. Univ. of Arizona Press, Tucson, p. 619
- Hartmann L., Kenyon S. J., 1996, *ARA&A*, 34, 207
- Kenyon S. J., Hartmann L. W., Strom K. M., Strom S. E., 1990, *AJ*, 99, 869
- Larson R. B., 1969, *MNRAS*, 145, 271
- Machida M. N., Inutsuka S., Matsumoto T., 2006, *ApJ*, 647, L151
- Machida M. N., Inutsuka S., Matsumoto T., 2010, *ArXiv e-prints*
- Machida M. N., Matsumoto T., Hanawa T., Tomisaka K., 2005, *MNRAS*, 362, 382
- Masunaga H., Inutsuka S.-I., 2000, *ApJ*, 531, 350
- Morris J. P., Monaghan J. J., 1997, *J. Comp. Phys.*, 136, 41
- Norman M. L., Wilson J. R., 1978, *ApJ*, 224, 497
- Pollack J. B., McKay C. P., Christofferson B. M., 1985, *Icarus*, 64, 471
- Price D. J., 2007, *Publ. Astron. Soc. Australia*, 24, 159
- Price D. J., Bate M. R., 2007, *MNRAS*, 377, 77
- Price D. J., Monaghan J. J., 2005, *MNRAS*, 364, 384
- Price D. J., Monaghan J. J., 2007, *MNRAS*, 374, 1347
- Saigo K., Tomisaka K., 2006, *ApJ*, 645, 381
- Saigo K., Tomisaka K., Matsumoto T., 2008, *ApJ*, 674, 997
- Scott E. R. D., 2007, *Ann. Rev. Earth Planet. Sci.*, 35, 577
- Stamatellos D., Whitworth A. P., Bisbas T., Goodwin S., 2007, *A&A*, 475, 37
- Tomida K., Tomisaka K., Matsumoto T., Ohsuga K., Machida M. N., Saigo K., 2010, *ArXiv e-prints*
- Tscharnutter W. M., 1987, *A&A*, 188, 55
- Tscharnutter W. M., Schönte J., Gail H., Tieloff M., Lüttjohann E., 2009, *A&A*, 504, 109
- Vorobyov E. I., Basu S., 2005, *ApJ*, 633, L137
- Vorobyov E. I., Basu S., 2006, *ApJ*, 650, 956

Whitehouse S. C., Bate M. R., 2006, MNRAS, 367, 32

Whitehouse S. C., Bate M. R., Monaghan J. J., 2005, MNRAS,  
364, 1367

Zhu Z., Hartmann L., Gammie C., 2009, ApJ, 694, 1045